Vol 18 No 9, September 2009
1674-1056/2009/18(09)/4030-07

Chinese Physics B

© 2009 Chin. Phys. Soc.
and IOP Publishing Ltd

Upconversion emission enhancement of TiO_2 coated lanthanide-doped Y_2O_3 nanoparticles

Lü Qiang(吕 强)[a)b)†], Zhao Lian-Cheng(赵连城)[a)],
Guo Feng-Yun(国凤云)[a)], and Li Mei-Cheng(李美成)[a)]

[a)] *Department of Material Physics and Chemistry, School of Material Science and Engineering, Harbin Institute of Technology, Harbin* 150001, *China*
[b)] *Center of Electron Microscope Technology, Mudanjiang Medical College, Mudanjiang* 157011, *China*

(Received 12 November 2007; revised manuscript received 15 November 2008)

To investigate the upconversion emission, this paper synthesizes Tm^{3+} and Yb^{3+} codoped Y_2O_3 nanoparticles, and then coats them with TiO_2 shells for different coating times. The spectral results of TiO_2 coated nanoparticles indicate that upconversion emission intensities have respectively been enhanced 3.2, 5.4, and 2.2 times for coating times of 30, 60 and 90 min at an excitation power density of 3.21×10^2 W·cm^{-2}, in comparison with the emission intensity of non-coated nanoparticles. Therefore it can be concluded that the intense upconversion emission of Y_2O_3:Tm^{3+}, Yb^{3+} nanoparticles can be achieved by coating the particle surfaces with a shell of specific thickness.

Keywords: upconversion emission, nanoparticle, Tm^{3+} and Yb^{3+} codoped, Y_2O_3 TiO_2 shell
PACC: 8140T, 3250, 7855, 7865M

1. Introduction

In recent years, upconversion luminescence of lanthanide-doped nanoparticles has attracted a great deal of attention due to their unique optical properties and potential applications in some fields, such as solid state lighting,[1] display monitors,[2] optical communications[3,4] and biological fluorescence labels.[5−7] However, a precondition for the development of lanthanide-doped nanoparticles as fluorescence biolabels is to obtain water-soluble, photostable and biocompatible nanoparticles. Unfortunately, most inorganic nanoparticles doped with lanthanide ions are hydrophobic. A convenient strategy for introducing or grafting hydrophilic/active functional groups onto nanoparticle surfaces can resolve the problem.[8−10] Due to the well-known silica surface chemistry and its benign effects in biological systems, silica-coated shells are usually considered for precoating the particle surfaces in order to further functionalize with active functional groups on silica shell surfaces.[11−13] In addition, TiO_2 is also one of the suitable candidates for shell materials due to its high transparency in the visible wavelength region and its good thermal, chemical, and mechanical properties.[14,15] Nevertheless, upconversion emission of TiO_2 coated lanthanide-doped nanoparticles has been rarely reported.

Another precondition for lanthanide-doped nanoparticles as biolabels is that upconversion emission intensities of the doped nanoparticles before and after coating shells cannot be dramatically weakened. Fortunately, the Haase group[16] recently reported an improvement in quantum yield after coating a $LaPO_4$ shell on a $CePO_4$:Tb core. Moreover, investigators have also focused on the enhancements of luminescence and upconversion emissions for the coated nanoparticles, such as silica-coated Ln^{3+}-doped LaF_3,[12] surface modified LaF_3/Ln, $LaPO_4$/Ln[17] and $NaYF_4$:Er(Tm),Yb/$NaYF_4$/polymer.[18] Here, we report the coating of Y_2O_3:Tm^{3+}, Yb^{3+} nanoparticles with TiO_2 shells using the Stöber method. According to the upconversion emission intensities of TiO_2 coated nanoparticles, a competitive mechanism between two components is presented. One component is the role conversion from the 'dormant' state to the 'activated' state of lanthanide ions on particle surfaces due to the effects of TiO_2 coated shells. Another component is the absorption effect of TiO_2 shells on incident pump light and the reabsorption effect of TiO_2 shells on upconversion emission. Enhancements in the upconversion emission intensities

†Corresponding author. E-mail: qianglu@yahoo.cn

of TiO_2 coated nanoparticles are demonstrated by using the competitive mechanism.

2. Experiment

Tm^{3+} and Yb^{3+}codoped Y_2O_3 nanoparticles were synthesized according to the procedure[19,20] with a slight modification as follows: appropriate amounts of high purity Tm_2O_3, Yb_2O_3 and Y $(NO_3)_3{\cdot}6H_2O$ with a corresponding mole ratio of cations were fully dissolved in dilute nitric acid solution (1:1 by volume). Citric acid (0.33 mol), glycol (1.6 mol), and polyethylene glycol 20000 (2.7×10^{-4} mol) were added, respectively. The turbid suspension was heated at 80 °C and stirred for 8 h to form a gel. The obtained gel was preheated at 300 °C for 1 h, and then sintered at 800 °C for 1 h in air to remove organic materials and form final powder samples. Moreover, according to the modified Stöber method, powder samples as core and isopropyl alcohol as solvent were added into the flask. Powder samples were dispersed with ultrasonic oscillation for 30 min. Deionized water and hydrous ammonia (25%) were added. After strong stirring at 34 °C for 10 min, butyl titanate was also added. Under the same conditions, the reaction continued for 30, 60 and 90 min, respectively. The precipitate was then centrifuged, washed and dried at 80 °C for 24 h.

The x-ray diffraction pattern recorded by a Rigaku D/max-γB diffractometer shows that the crystal structure of the prepared powders is cubic. The powder morphologies and TiO_2 shell thicknesses were observed by using a JEOL-1010 transmission electron microscope (TEM, accelerating voltage 100 KV, resolution of point image 0.4 nm). Upconversion emission was carried out under a diode laser excitation (976.1±2.9 nm, 1.3 W, continuous wave with 1 m fibre (NA: 0.22 and Ø100 μm), Beijing Hi-Tech Optoelectronics Co., Ld. China). Fluorescence was collected with a Hitachi F-2500 fluorescence spectrophotometer (instrument parameters: 2.5 nm for excitation slit; 2.5 nm for emission slit; 400 V for PMT voltage and 0.08 s for response) under 25.2 mW (3.21×10^2 W$\cdot$cm^{-2}) excitation at room temperature.

3. Results and discussion

The upconversion emission spectra of non- and TiO_2-coated Y_2O_3:Tm^{3+}, Yb^{3+} nanoparticles are shown in Fig.1, irradiated under an excitation power density of 3.21×10^2 W$\cdot$cm^{-2} with a 976 nm diode laser. Since the upconversion emission spectra for all samples manifest characteristics which are similar to each other, it is reasonable to ascribe the upconversion emissions to the same origins. The upconversion emission bands at 477 and 489 nm originate radiative transitions from the Tm^{3+} lowest Stark sublevel $^1G_4$ to different Stark sublevels $^3H_6$.

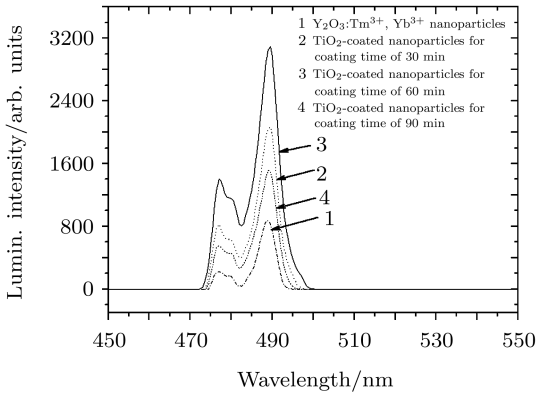


Fig.1. Upconversion emission spectra of non- and TiO_2 coated Y_2O_3:Tm^{3+}, Yb^{3+} nanoparticles for sintered time of 60 min at 800 °C and coating times of 30, 60 and 90 min. All samples are excited at 25.2 mW (3.21×10^2 W$\cdot$cm^{-2}) at room temperature.

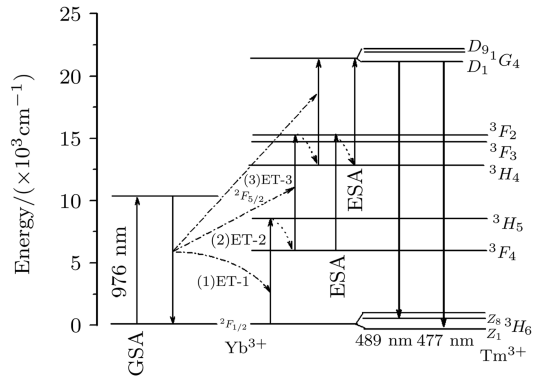


Fig.2. Energy level diagrams of Tm^{3+} and Yb^{3+} ions with Stark splitting in cubic Y_2O_3:Tm^{3+}, Yb^{3+} nanoparticles, and upconversion mechanism.

The upconversion mechanism is attributed to a successive three-step energy transfer or three-photon process from three excited Yb^{3+} ions nearby to one Tm^{3+} ion, which is shown in detail in Fig.2. At the same time, for a few excited states, absorption of Tm^{3+} ion takes place from level $^3F_4$ to $^3F_2$ and from level $^3H_4$ to $^1G_4$. In addition, phonons are also needed because the energy transfer from Yb^{3+} ions to Tm^{3+} ions is not a complete resonance according to

their energy levels. For an unsaturated upconversion emission process, upconversion emission intensity $I_{\rm up}$ depends on incident pump power $I_{\rm pump}$ according to the relation $I_{\rm up} \propto I_{\rm pump}^{n}$, where n is the number of photons involved in the pumping process.[21]

To verify the three-photon upconversion mechanism, the laser pump power dependences of the upconversion radiations are measured and displayed in Fig.3. The slopes of the double logarithmic fitted lines are close to 3, indicating that blue upconversion emissions of non- and TiO_2-coated Y_2O_3:Tm^{3+}, Yb^{3+} nanoparticles indeed are a three-photon excitation process.

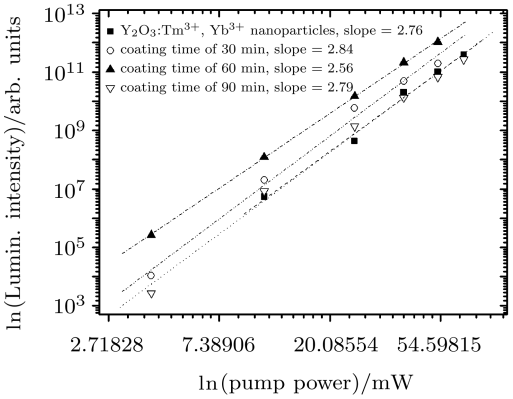


Fig.3. The integrated intensities of upconversion emissions of non- and TiO_2 coated Y_2O_3:Tm^{3+}, Yb^{3+} nanoparticles as a function of laser pump power.

It is well known that electric dipole transitions of lanthanide ions between intra-$4f^n$ states are dominant because the line strengths of electric dipole transitions are much stronger than those of electric quadrupole transitions and magnetic dipole transitions. Although electric quadrupole transitions and magnetic dipole transitions between intra-$4f^n$ states of the isolated lanthanide ions are allowed, electric dipole transitions are forbidden. So, direct excitation for the isolated lanthanide ions is a relatively inefficient process due to the forbidden character of electric dipole transitions between intra-$4f^n$ states. In comparison with the energy levels of the isolated lanthanide ions, the discrete energy levels of lanthanide ions in the host lattice can be perturbed by the crystalline field; this fact results in the decrease of the selection rule of radiation transition. Practically, the upconversion luminescence of lanthanide ions originates from intra-$4f^n$ transitions perturbed by static crystalline fields and does not involve valence electrons.[22,23] So, crystalline fields are a prerequisite for the upconversion luminescence of lanthanide ions. Due to numerous surface effects of nanoparticles, such as lattice distortion, broken bond and other surface defects, the crystalline fields on crystal–air interfaces are badly degenerated.[24−26] A lower quantum yield is consequently observed from the direct excitation process of the isolated lanthanide ions, and from lanthanide ions embedded on the particle surfaces due to less perturbation by the degenerated crystalline fields on the crystal–air interfaces. Based on the above viewpoint, the upconversion emissions of lanthanide-doped nanoparticles practically originate from lanthanide ions within nanoparticles rather than those on the particle surfaces. Fortunately, the coated shell structures can effectively decrease the surface effects and improve the degenerated crystalline fields between the core–shell interfaces.[27,28] The improved crystalline fields can split $^{2S+1}L_J$ levels of lanthanide ions between the core–shell interfaces into several Stark levels, and further mix their different J states to weaken the selection rules of radiation transitions. Consequently, large numbers of lanthanide ions between the core–shell interfaces can become new isolated luminescence centres; this fact obviously results in enhancements in the upconversion emission intensities of core–shell lanthanide-doped nanoparticles. A schematic diagram of lanthanide ions in the interior core, nearby, and on the core–shell interface is shown in Fig.4, where symbolic marks A and B show lanthanide ions in the interior; mark C indicates a lanthanide ion near the interface; mark D exhibits a lanthanide ion embedded on the crystal–air interface, which is called as the 'dormant' lanthanide ion; mark E represents a lanthanide ion coated by TiO_2 shells with thicknesses of d_1, d_2 and d_3, which is called as the 'activated' lanthanide ion because of having a new luminescence centre.

In our experiments, TiO_2 coated shells can be distinctly identified by TEM micrographs in Fig.5. However, x-ray diffraction (XRD) spectra of TiO_2 coated Y_2O_3:Tm^{3+}, Yb^{3+} nanoparticles in Fig.6 only show highly crystalline core structures. No characteristic diffraction peaks of crystalline TiO_2 shells are detected. Further experiments with pure TiO_2 fine powders synthesized under the same conditions confirm that the TiO_2 shells on the particle surfaces are non-crystalline, as shown in Fig.6(a).

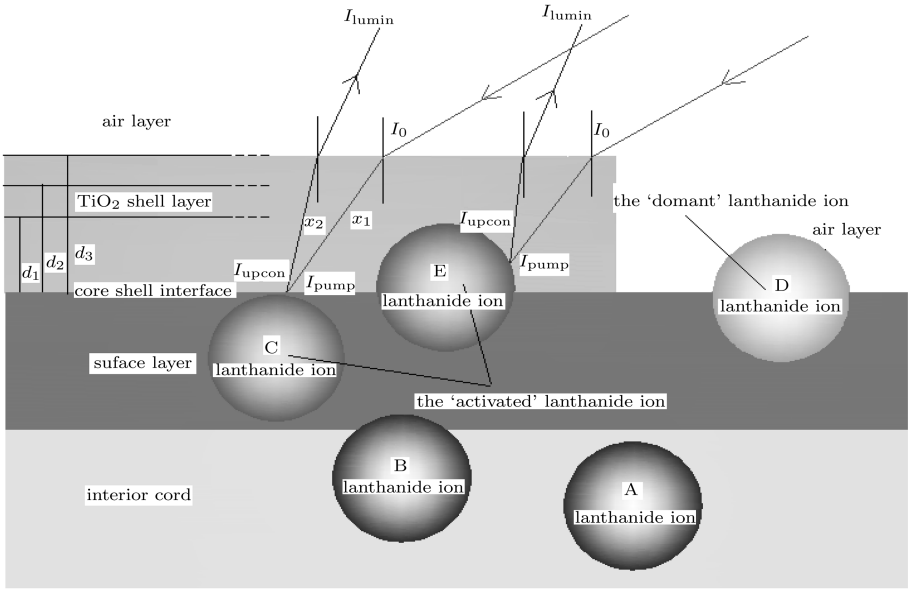


Fig.4. Schematic diagrams of lanthanide ions near, on the core–shell interface and in the interior core, as well as the absorption effects of TiO_2 shells on 980 nm incident light and reabsorption effects on 477 and 489 nm upconversion emission.

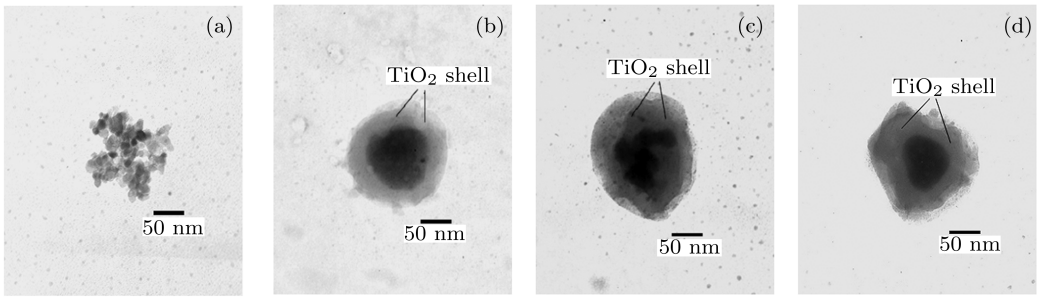


Fig.5. TEM micrographs of non-coated (a) and TiO_2 coated Y_2O_3:Tm^{3+}, Yb^{3+} nanoparticles for coating times of 30 (b), 60 (c) and 90 min (d).

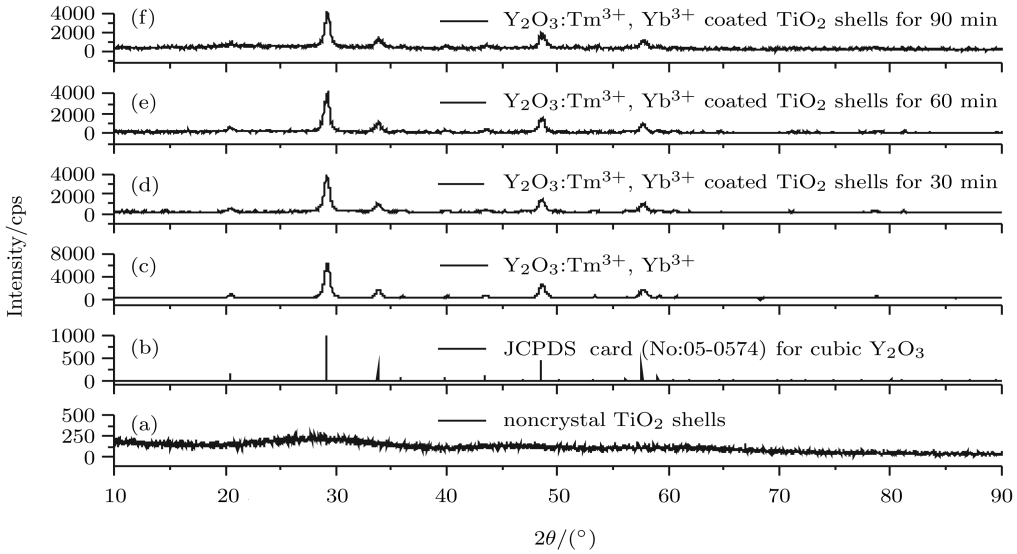


Fig.6. XRD spectra of noncrystalline TiO_2 shells (a), JCPDS card (No:05-0574) for cubic Y_2O_3(b),Y_2O_3:Tm^{3+}, Yb^{3+} nanoparticles (c) and TiO_2 coated Y_2O_3:Tm^{3+}, Yb^{3+} nanoparticles for coating times of 30 (d), 60 (e) and 90 min (f).

After coating with noncrystalline TiO_2 shells, intra-4f^n states of lanthanide ions between the core–shell interfaces can be perturbed by a ligand field: one component is from the host, and the other from the noncrystalline TiO_2 shells. Consequently, lanthanide ions between the core–shell interfaces are activated to participate in the upconversion emission process. Thus, the enhancements of the upconversion emission intensities for TiO_2 coated with Y_2O_3:Tm^{3+}, Yb^{3+} nanoparticles should be considered as contributions from lanthanide ions on the particle surfaces, i.e. role conversion of lanthanide ions on the particle surfaces from the 'dormant' state to the 'activated' state. This means that noncrystalline TiO_2 coated shells indeed provide the 'dormant' lanthanide ions on the particle surfaces with ligand fields to activate them, leading to an additional upconversion emission. Moreover, the enhanced degrees of upconversion emission intensities of the coated nanoparticles should be determined by some factors, such as lanthanide-doped concentrations, specific surface areas of nanoparticles, different shell materials and the coated shell thicknesses.

In comparison with the upconversion emission intensity of non-coated nanoparticles in our experiments, 3.2, 5.4, and 2.2 times enhancements of the upconversion emission intensities of TiO_2 coated with Y_2O_3:Tm^{3+}, Yb^{3+} nanoparticles for coating times of 30, 60 and 90 min are respectively observed at an excitation power density of 3.21×10^2 W$\cdot$cm^{-2}. To enable quantitative evaluation of the effects of shell thicknesses on the additional upconversion emission intensities, a parameter called relative variable ratios (RVR) of upconversion emission intensities is introduced here. Thus, RVR is defined as

$$\mathrm{RVR} = \frac{I_{\mathrm{coat}} - I_{\mathrm{ref}}}{I_{\mathrm{ref}}} \times 100\%, \tag{1}$$

where I_{coat} and I_{ref} are the integrated intensities of upconversion emission of TiO_2 coated and non-coated nanoparticles as references, respectively. From the calculated results of RVR in Table 1, it can be seen that RVR begins to rapidly rise from a coating time of 30 to 60 min, and then undergoes an abrupt reversal at 60 min, subsequently falling from 60 to 90 min sharply. The developing tendency of RVR implies that besides role conversion of lanthanide ions on the particle surfaces, another factor has practically influenced the upconversion emission enhancements of TiO_2 coated nanoparticles with increasing shell thicknesses.

Table 1. Relative variable ratios of upconversion emission integrated intensities of TiO_2 coated Y_2O_3:Tm^{3+}, Yb^{3+} nanoparticles for different coating times. All samples are excited at 25.2 mW (3.21×10^2 W$\cdot$cm^{-2}) at room temperature.

coating time	30 min	60 min	90 min
RVR	223.1%	444.3%	123.2%

Considering the same upconversion material used in our experiments, we find that the factor should result from absorption effects of TiO_2 shells on incident light. According to Lambert's law,[29] transmission intensities of incident light will decrease with increasing absorption layer thicknesses, namely

$$I_{\mathrm{trans}} = I_0 \mathrm{e}^{-kx}, \tag{2}$$

where I_{trans} is the transmission intensity; I_0 is the incident light intensity; k is the absorption coefficient of solid; x is the transmission distance of incident light in a solid. In addition, the absorption coefficient of the solid is related to both the refractive index and the extinction coefficient of the solid according to Ref.[29], namely

$$k = \frac{4\pi}{\lambda_0} n_{\mathrm{re}} \eta, \tag{3}$$

where λ_0 is the wavelength of incident light; n_{re} is the refractive index of the solid; η is the extinction coefficient of the solid. Because the transmission light is also the pump light in Fig.4, the absorption effects of different thickness TiO_2 shells on 976 nm incident light actually weaken the pump light, and further decrease the upconversion emission intensities of TiO_2 coated nanoparticles according to the relation $I_{\mathrm{up}} \propto I_{\mathrm{pump}}^n$. Moreover, reabsorption effects of TiO_2 shells on 477 and 489 nm upconversion emissions also should be considered. Assume that the transmission distances (x) of incident light can be substituted by TiO_2 shell thicknesses, which are measured from TEM micrographs in Fig.5. The refractive index of TiO_2 film is 2.30 at 500 nm,[30] and its extinction coefficient is about 7.5×10^{-4}; the refractive index of TiO_2 film is 2.09∼2.31 at 980 nm,[31] and its extinction coefficient is about $2.0\times10^{-2} \sim 3.5\times10^{-2}$. According to Eqs.(2), (3), and the relation $I_{\mathrm{up}} \propto I_{\mathrm{pump}}^n$, we can calculate the influence of different thickness TiO_2 shells on 980 nm incident light and 500 nm upconversion emission, as shown in Table 2. It can be seen from the calculated results that the thicker TiO_2 shells are, the stronger

both absorption effects of TiO_2 shells on 980 nm incident light and reabsorption effects on 500 nm upconversion emissions are. Thus, we ascribe the upconversion emission enhancements of TiO_2 coated nanoparticles to a competition process between two mechanisms. The first is the role conversion of lanthanide ions on the particle surfaces from the 'dormant' state to the 'activated' state due to re-perturbation by the ligand fields from coating noncrystalline TiO_2 shells. The other is the absorption effects of different thickness TiO_2 shells on incident pump light and reabsorption effects of TiO_2 shells on the upconversion emission. When the TiO_2 shells are thinner, the enhancements in the upconversion emission intensities of TiO_2 coated nanoparticles originating from role conversion of lanthanide ions on the particle surfaces are predominant, while absorption and reabsorption effects of TiO_2 shells are also weak; this fact leads to the enhancements in upconversion emission of TiO_2 coated nanoparticles. When TiO_2 shells are thick, absorption and reabsorption effects of TiO_2 shells turn into the dominant factor in the competition process; this fact obviously weakens the upconversion emission of TiO_2 coated nanoparticles. It is a specific thickness TiO_2 shell that can provide the best ligand field for the 'dormant' lanthanide ions on the particle surfaces to fully activate them, and absorption and reabsorption effects of TiO_2 shells are also appropriate; this fact results in the remarkable enhancements in upconversion emission of TiO_2 coated nanoparticles.

Table 2. Absorption effects of different thickness TiO_2 shells on 980 nm incident light, upconversion emission and reabsorption effects of TiO_2 shells on 500 nm upconversion emission.

coating time	30 min	60 min	90 min
TiO_2 shell thickness	34 nm	50 nm	63 nm
absorption effects of TiO_2 shells on 980 nm incident light (I_{pump} / I_0)	96.8%	95.3%	94.2%
$I_{\mathrm{up}} \propto I^n_{\mathrm{pump}}(I_{\mathrm{up}}/I^3_0, n = 3)$	90.7%	86.6%	83.6%
reabsorption effects of TiO_2 shells on 500 nm upconversion emission (I_{lumin}/I^3_0)	90.6%	86.4%	83.4%

4. Conclusions

It can be seen from the above results and discussion that the upconversion emission intensities of Y_2O_3:Tm^{3+}, Yb^{3+} nanoparticles can be enhanced by coating with TiO_2 shells. In comparison with the upconversion emission intensity of non-coated nanoparticles, 3.2, 5.4, and 2.2 times enhancements of the upconversion emission intensities of TiO_2 coated Y_2O_3:Tm^{3+}, Yb^{3+} nanoparticles for coating times of 30, 60 and 90 min can be respectively achieved at an excitation power density of 3.21×10^2 W$\cdot$cm^{-2}. Considering the developing tendency of RVR, a competition process between two mechanisms was presented. It can be therefore concluded that intense upconversion emission of Y_2O_3:Tm^{3+}, Yb^{3+} nanoparticles can be achieved by coating the surfaces of doped nanoparticles with a specific thickness shell.

References

[1] Lu C H, Hong H C and Jaganathann R 2002 *Mater. Chem.* **12** 2525

[2] Mehta A, Thundat T, Barnes M D, Chhabra V, Bhargava R, Bartko A P and Dickson R M 2003 *Appl. Opt.* **42** 2132

[3] Zhang H X, Kam C H, Zhou Y, Han X Q, Buddhudu S, Xiang Q, Lam Y L and Chan Y C 2000 *Appl. Phys. Lett.* **77** 609

[4] Patra A, Friend C S, Kapoor R and Prasad P N 2002 *J. Phys. Chem.* B **106** 1909

[5] Bruchez M, Moronne M, Gin P, Weiss S and Alivisatos A P 1998 *Science* **281** 2013

[6] Stephan H, Karsten K, Hans U G and Markus H 2004 *Adv. Mater.* **23-24**(16) 2101

[7] Wang L, Yang C Y and Tan W H 2005 *Nano Lett.* **5** 37

[8] Andrea Schroedter, Horst Weller, Ramon Eritja, William E Ford and Jurina M Wessels 2002 *Nano Lett.* **2**(12) 1363

[9] Rahul P Bagwe, Lisa R Hilliard and Tan W H 2006 *Langmuir* **22** 4357

[10] Christopher A Traina and Jeffrey Schwartz 2007 *Langmuir* **23** 9158

[11] Ji J M, Chen Y D, Robert A S and Jeffery L C 2001 *Chem. Mater.* **13** 4783

[12] Sivakumar S, Diamente P R and Veggel F C J M V 2006 *Chem. Eur. J.* **12** 5878

[13] Li Z Q and Zhang Y 2006 *Angew. Chem. Int. Ed.* **45** 7732
[14] Li J G, Wang X H, Kenji Watanabe and Takamasa Ishigaki 2006 *J. Phys. Chem.* B **110** 1121
[15] Bai L Y, Su X Y and Lei M K 2006 *J. Inorg. Mater.* **21**(5) 1085
[16] Kömpe K, Borchert H, Storz J, Lobo A, Adam S, Möller T and Haase M 2003 *Angew. Chem. Int. Edit.* **42** 5513
[17] Stoudam J W and Veggel F C J M V 2004 *Langmuir* **20** 11763
[18] Yi G S and Gan-Moog Chow 2007 *Chem. Mater.* **19**(3) 341
[19] Cushing B L, Kolesnichenko V L and O'Connor C J 2004 *Chem. Rev.* **104** 3893
[20] Lin C K, Zhang C M and Lin J 2007 *J. Phys. Chem.* C **111** 3300
[21] Yu Y, Lü S C, Zhou B B and Xin X S 2006 *Acta Phys. Sin.* **55**(8) 4332 (in Chinese)
[22] Judd B R 1962 *Phys. Rev.* **127**(3) 750
[23] Ofelt G S 1962 *J. Chem. Phys.* **37** (3) 511
[24] Peng H S, Song H W, Chen B J, Lü S Z and Huang S H 2003 *Chem. Phys. Lett.* **370** 485
[25] Peng H S, Huang S H, Sun L D and Yan C H 2007 *Phys. Lett.* A **367** 211
[26] Lou W X, Huang S H, You F T and Peng H S 2007 *Acta Phys. Sin.* **56**(3) 1765 (in Chinese)
[27] Feng H J, Chen Y, Tang F Q and Ren J 2006 *Mater. Lett.* **60** 737
[28] Lü Q, Li A H, Guo F Y, Sun L and Zhao L C 2008 *Nanotechnology* **19** 205704
[29] Mu G G and Zhan L Y 1978 *Optics* (Beijing: People Education Press) p537 (in Chinese)
[30] Yao J K, Fan Z X, Jin Y X, Zhao Y N, He H B and Shao J D 2008 *Thin Solid Films* **516** 1237
[31] Jiang H Q, Wei Quan, Cao Q X and Yao Xi 2008 *Ceramics International* **34** 1039